IEEE Access
Multidisciplinary | Rapid Review | Open Access Journal

Received September 23, 2019, accepted October 8, 2019, date of publication October 14, 2019, date of current version October 23, 2019.

Digital Object Identifier 10.1109/ACCESS.2019.2947160

Olive-Fruit Variety Classification by Means of Image Processing and Convolutional Neural Networks

JUAN M. PONCE, ARTURO AQUINO, AND JOSÉ M. ANDÚJAR, (Senior Member, IEEE)

Department of Electronic Engineering, Computer Systems and Automation, Higher Technical School of Engineering, University of Huelva, 21007 Huelva, Spain

Corresponding author: Juan M. Ponce (jmponce.real@diesia.uhu.es)

This work was supported in part by the INTERREG Cooperation Program V-A SPAIN-PORTUGAL (POCTEP) 2014–2020, and in part by the ERDF funds within the scope of the TecnOlivo Project under Grant 0155_TECNOLIVO_6_E.

ABSTRACT The automation of classification and grading of horticultural products attending to different features comprises a major challenge in food industry. Thus, focused on the olive sector, which boasts of a huge range of cultivars, it is proposed a methodology for olive-fruit variety classification, approaching it as an image classification problem. To that purpose, 2,800 fruits belonging to seven different olive varieties were photographed. After processing these initial captures by means of image processing techniques, the resulting set of images of individual fruits were used to train, and continuedly to externally validate, the implementations of six different Convolutional Neural Networks architectures. This, in order to compute the classifiers with which perform the variety categorization of the fruits. Remarkable hit rates were obtained after testing the classifiers on the corresponding external validation sets. Thus, it was yielded a top accuracy of 95.91% when using the Inception-ResnetV2 architecture. The results suggest that the proposed methodology, once integrated into industrial conveyor belts, promises to be an advanced solution to postharvest olive-fruit processing and classification.

INDEX TERMS Computer vision, convolutional neural network, fruit variety, food industry, fruit classification, image processing, olive.

I. INTRODUCTION

Olive (Olea europaea L.) growing is currently an agronomic activity of great importance. With an ancient tradition throughout the Mediterranean basin, its cultivation has spread around the world in recent decades [1], [2], and consumption of table olives and olive oil, which are the most important products derived from this crop, have exploded. Indeed, in accordance with the International Olive Council (IOC), the consumption of table olives has more than doubled in the past 20 years [3], with an estimation of 2,667,000 tonnes in 2018/19 against the 1,185,500 tonnes consumed worldwide during the year 1998/1999. In the case of olive oil, the numbers are equally significant, and in the same 20-year period its consumption has increased in more than 500,000 tonnes, being estimated 2,950,500 tons for the year 2018-19 [4].

Therefore, and as it is happening with other mainstream crops, the olive sector has to face multiple challenges in order to satisfy this high demand market, in which the popularity of olive-derived products does not stop growing. Increasing production while reducing the associated costs, and all this in an environmentally sustainable way, is a cross-cutting problem in current agriculture [5]–[7]. The introduction of new technologies is playing a fundamental role to deal with this situation. And this is happening in virtually every scope related to agricultural activities. In this sense, postharvest tasks have become an important spotlight. Indeed, optimising processes involved in the treatment and manipulation of horticultural products, once they are gathered, may have a remarkable cost-saving impact [8].

Within this context, postharvest classification of horticultural products, according to different features such as size or surface condition, has become a main focus of research. This, since it has been traditionally performed manually, implying tedious, inaccurate and time-consuming tasks. Hence, its automation has become a major problem in food industry. The case of olive sector is not an exception, as postharvest fruit classification remains a challenge for olive growers.

The associate editor coordinating the review of this manuscript and approving it for publication was Gianluigi Ciocca.

Thus, while the automation of the olive-fruit size grading has historically found different solutions, all of them usually based on mechanical approaches, the classification according different criteria, with a potential value for farmers and producers, is still attached to manual inspection. This may be the case of individually classifying olive fruits according to their variety, feature in which the present study is focused on. By not discriminating among varieties when gathering the olive-fruits, harvest costs can be potentially reduced. It should be noted that harvesting is a key factor for olive growing, obviously directly related to the prize of the eventual product, and with a critical impact in the productivity and viability of olive growing as a business. Therefore, olive sector has put huge efforts to improve and optimise harvesting. New orchards planning or harvesting mechanization are some of the advances introduced during the last few decades in order to enhance fruit gathering [9], [10]. Indirectly, it may benefit from a postharvest automated classification system to separate the fruits, once they have been transported to the mill, according their variety. This could ease optimise harvesting, when orchards are shared by different varieties of olive-trees, not being necessary to consider this circumstance when planning the collection of the fruits.

Machine Vision systems, commonly used in a great variety of industries, have become familiar within the food sector, when inspecting and supporting the automatic handling of commodities [11]. By their integration throughout the manipulation process, the products to handle can be imaged, and descriptive features of each of them can be extracted in real time, via image processing and analysis. This information can be potentially used to label or categorize each of these products, according to models previously computed. So, this technology sets itself up as a potential solution to the automation of the olive-fruit variety-based classification.

In recent years, Computer Vision has significantly benefited from the recent revitalisation of Deep Learning, which has seen increased its popularity and it has experienced an exponential growth, both in terms of the amount of related research conducted and its applications. This sort of subset of machine learning methods is nothing new, and the principles it is based on have been around for a while [12], [13]. Nevertheless, the increase of computational power provided by graphics processing units (GPUs) [14], along with the huge amount of data offered by the Internet [15], have been seen as an opportunity to boost Deep Learning performance. Within this field, Convolutional Neural Networks (CNN) has supposed a breakthrough in image processing and analysis, and nowadays it comprises the main framework for image classifiers development and pattern recognition. Its applications have reached innumerable fields, ranging from the automotive industry, supporting self-driving cars [16]–[18], to the healthcare sector, with automatic diagnostic systems for the analysis of medical images [19], [20]. Smart farming and food sector are not an exception. Thus, over the past few years it has been published a considerable amount of literature related to the potential application of Deep Learning-based technologies to agriculture and food industry [21], [22]. Yield prediction [23]–[26], leaf defoliation estimation [27] or fruits and crops classification [11], [28]–[31] are just some examples of scopes within which the use of Deep Learning and CNNs has been explored.

Olive sector can potentially gain from the use of Deep Learning based-computer vision systems too. Hence, the main goal of this study is to assess the viability of performing a machine vision- and Deep Learning-based classification of olive-fruits according to their variety. To the best to authors' knowledge, the approach, methodology and results derived from this work are unseen in the literature to date. Whilst most research related to this topic draws on images of the endocarps of the fruits to that end [32]–[34], the methodology proposed here is focused on a non-invasive approach, in which the classification is carried out uniquely using the morphology of the olive-fruits as distinguishing feature. For that purpose, batches of fruits, stochastically disposed, were photographed inside an image acquisition chamber designed to be potentially integrable in current conveyor belts. Then, the initial captures were transformed by means of mathematical morphology and global thresholding techniques, obtaining a set of images of individual fruits. Next, different architectures of CNN were tried by training them with these images. Finally, the resulting classifiers were tested by using an external validation set to evaluate and compare their performance.

The present manuscript is organized as follows. First, section II overviews the fundamentals of CNNs as well as briefly describes the architectures of interest for this work. Section III-A specifies the olive varieties considered in the research, as well as different aspects related to fruit sample collection for configuring the data of study. Then, all aspects involved in the process of image acquisition are detailed (section III-B). Section III-C focuses on the framework employed to implement the proposed algorithms for image classification, emphasizing the different developing tools and technologies used. In section IV-A it is described the methodology to transform the initial captures into the individual fruit images that, as raw data, are used to try the different CNN architectures considered. CNN training and validation is detailed throughout sections IV-B-2 and IV-B-3, respectively. Section V exposes and discusses the results after validating the different image/olive-fruit-variety classifiers developed. Finally, section VI comprises the summary of the most relevant aspects concluded throughout the experimentation.

II. OVERVIEW OF CNN ARCHITECTURES

In the present study, olive-fruit classification is approached as an image classification problem, faced by means of machine learning, by using CNNs. Indeed, the irruption of Deep Learning as a mainstream technology has exploded in numerous and uneven domains [35], being Computer Vision a highly benefited niche [36], where CNNs have provided outstanding advances in the state of the art.

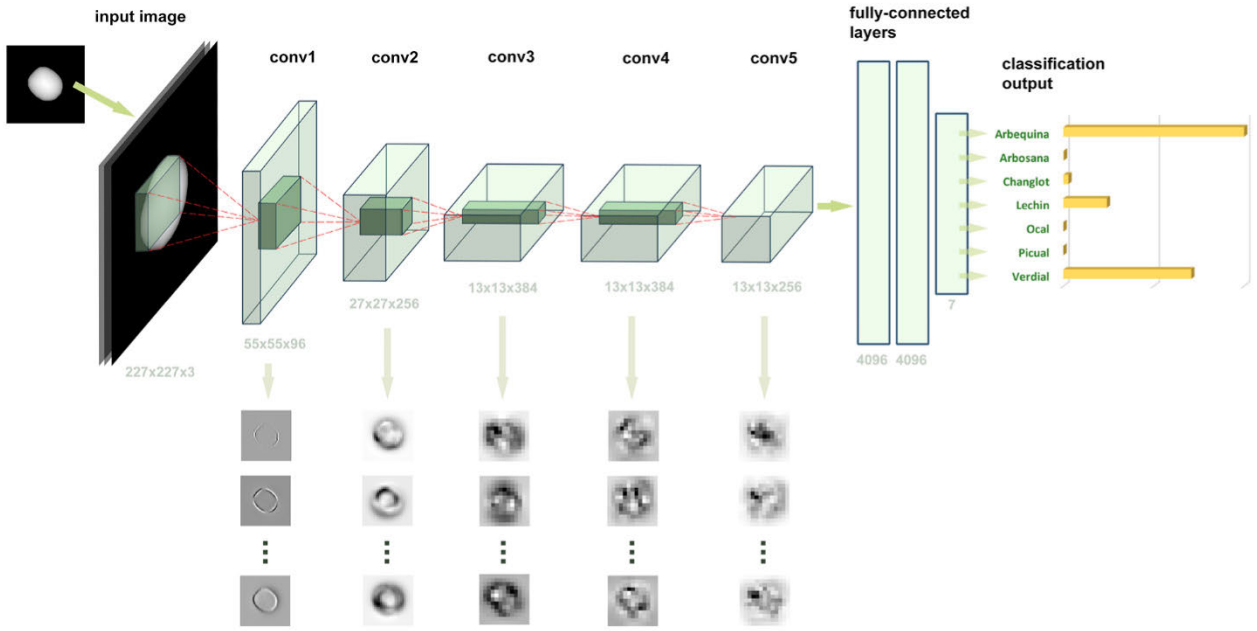

FIGURE 1. Schematic illustration of the performance of a CNN, with five convolutional layers, in determining the variety of an olive fruit. The input is an olive-fruit image resulting from the pre-processing described in section IV-A. The image feeds the net and passes through the convolutional layers, which model the object from the gross distinctive features to the subtle ones as the image goes deeper. Finally, the extracted features are processed by a fully connected layer which yields a probability for the object to belong to the considered classes. In this example, the olive fruit is classified as ***Arbequina***.

Due to improvements in the design and manufacturing of specialized-in-parallel-computing integrated circuits, and the introduction of standardised architectures such as CUDA, GPUs have become an affordable and powerful framework for general purpose processing. This opened up a window of opportunity for researchers and engineers to face tasks that were not possible before because of the non-assumable computational cost. In addition, public datasets for machine learning purposes has increased in number over the past few years. Thus, different initiatives, such as ImageNet [37] or CIFAR-10 [38] among lots of others, have made available huge quantities of quality data. This without taking into account the exorbitant amount of information privately handled by the big players in the technology industry such as Amazon, Baidu, Facebook, Google or Microsoft, which far from being outsiders of this trend, have become in actual boosters of Deep Learning and its applications [15], [39].

Notwithstanding the computational improvements and data availability, classical approaches using neural networks dealt with the difficulty of finding and designing a set of significant mathematical descriptors [40] to feed the net with, in order to solve a specific problem. In contrast, the irruption of CNNs has supposed a game-changer in Computer Vision, as these networks can be directly fed with image-corresponding pixel-intensity matrixes. Thus, a CNN is basically a Deep Neural Network where, layer by layer, this raw data provided by the initial image, is transformed into a set of high-level features which are eventually used to realise the classification. To that end, CNN architectures are usually shaped by three different types of layers: convolutional layers in which filters or kernels, acting as feature detectors, are convolved over local regions of the input; pooling layers, where it is reduced the spatial dimensionality of the convolved features (also known as activation maps) obtained after a convolution stage; and fully-connected layers, with which, and by using the high-level features obtained by convolution and down-sampling, the class scores are calculated, and therefore the image classification is performed (see Fig. 1). Because of its demonstrated virtues, which include reduced complexity, faster model training, capacities of capturing local information, smaller sample volume requirements or lower overfitting probability, researchers have shown an increased interest, and CNNs applications and related literature [35], [36], [39], [41], that is encouraged to be consulted for deeper study, have exploded in recent years.

For the purpose of developing a set of models to undertake the olive-fruit variety classification, some of the most important CNN architectures seen in recent years are considered; they are briefly described hereafter.

AlexNet [42] supposed a breakthrough within the image recognition scope. It is based on an 8-layer architecture, consisting of 5 convolutional layers and 3 fully connected ones. So, deeper when compared to the standards of that time, another of its contributions was to model the output of the neurons in the network with a Rectified Linear Unit (ReLU), instead of other more conventional activation functions, like tanh or sigmoid. Thanks to that, the CNN could be trained much faster.

InceptionV1 [43], as well known as GoogLeNet, imposes 1×1 convolutions in the middle of the network, and proposes a global average pooling at the end of it, as a substitute for a last fully connected set of neurons as an output. Very deep when compared to AlexNet, the first iteration of the Inception architecture comprises 22 layers in total.

InceptionV3 [44] reduces the number of parameters in the network by factorizing convolutions. This, by increasing the number of layers (up to 42 in total) and reducing the dimensions of the filters, without loss of efficiency.

ResNet [45] implies a paradigm shift, introducing the notion of skip (or shortcut) connection. The layer inputs do not just depend on the outputs of the immediate previous layer. This, in order to solve a major problem with gradient-based learning methods, the vanishing/exploding gradients [46], [47]. Its architecture is complemented with a bottleneck design which allows to reduce complexity without significantly impoverishing performance. In this case, different alternatives can be found regarding the depth of the network: ResNet-50, with 50 layers; ResNet-101 with 101 layers; ResNet-152 with 152 layers.

Inception-ResNetV2 [48], based on the Inception architecture, but inspired by ResNet, is trained with residual connections, allowing to speed up the process.

III. MATERIALS AND METHODS

A. SAMPLE COLLECTION

Seven different olive varieties were considered for this study: *Arbequina*, *Arbosana*, *Picual*, *Ocal*, *Changlot Real*, *Verdial de Huévar* and *Lechín de Sevilla*. For each of these cultivars, 400 fruits were handpicked in olive orchards located in Gibraleón (37°20'09.2''N 7°02'19.8''W), province of Huelva (Andalusia, Spain), in October 2018.

B. IMAGE ACQUISITION

For the purpose of capturing the images of the fruits, it was set up an ad-hoc image acquisition system, inspired in that proposed in [49]. The aim at this point was not to implement a final version of this device, integrable in a conveyor system, but a prototype mimicking its main features regarding image capture conditions. This system was conceived to acquire images with high contrast in terms of luminosity between the fruits and the background, with a shadowless lighting. This feature favours a subsequent stage of the experimentation, where a solid and accurate segmentation of the captures is necessary.

The ad-hoc image acquisition system was designed to be potentially integrable in a conveyor belt. It consists of four main parts: a chamber with which the capture area can be isolated from any external light pollution; a lighting system, based on seven equally distributed strips of 25 5V-LEDs each, located at the base of the chamber; a semi-translucent white plastic surface comprising the capture area, over which olive-fruits are placed to be photographed; a digital mirrorless camera mounted above the chamber, looking perpendicularly at the capture area. Fig. 2 illustrates the described system.

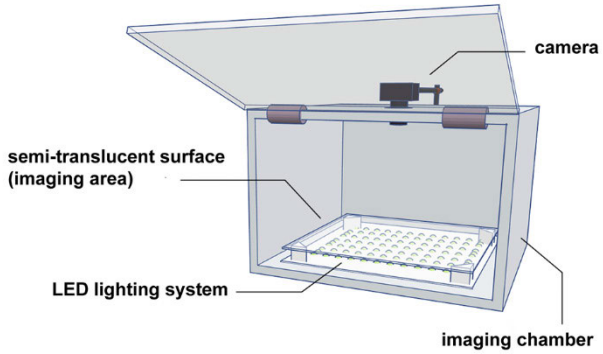

FIGURE 2. Image acquisition system.

FIGURE 3. Example of image acquired for Ocal variety.

It should be noted that the camera used for imaging the fruits, a Sony α7-II (Sony Corp., Tokyo, Japan), was equipped with a Zeiss 24/70mm lens (Carl Zeiss AG, Oberkochen, Germany) and configured in manual mode, with an aperture of f/7.1, shutter speed of 1/50s, focal length of 31mm and ISO sensitivity of 250. The initial captures were saved in JPEG format, with a resolution of 6000 $\times$ 3376 pixels and 24 bits of colour depth. The pixel density was set to 350ppi.

Every variety-set of 400 fruits was photographed in batches of 50 individuals, thus generating 8 images per variety. With the aim of mimicking a realistic scenario, it should be remarked that the fruits were stochastically placed on the capture area, with the only restriction of not appearing any of them touching the border in the resulting image. Fig. 3 shows an example of an image taken following the specified criteria.

C. IMAGE PROCESSING ALGORITHM IMPLEMENTATION AND CNN TRAINING/VALIDATION

The image processing algorithm, developed to transform the starting captures into the set of images to be used throughout the experimentation, was implemented with MATLAB and its Image Processing Toolbox, release 2018a (The MathWorks Inc., Natick, Massachusetts, USA). A MATLAB framework was also used in order to perform the training of the CNNs for image classification, and the validation of the results yielded by them. CNN training was conducted

FIGURE 4. Colour variability of four different olive-fruits, of the *Arbequina* variety, collected at the same time within the same orchard.

by transfer learning [19], so pre-trained implementations of the different CNN architectures approached in the present study (which will be later briefly described), available through the MATLAB Deep Learning Toolbox, were used.

The different networks tried were trained by GPU computing, using a single 8GB-NVIDIA GTX 1080 graphic card (Nvidia Corporation, Santa Clara, California, USA).

IV. DEVELOPED METHODOLOGY

A. IMAGE PRE-PROCESSING

As stated before, the main goal of the present study is to provide a computer-vision methodology for the individual classification of olive-fruits, according to their variety, present in images containing multiple individuals, even in touch. A first approach to the problem may consider colour characteristics as a feature to base the classification on. However, for the case of this crop, colour is known to be strongly dependent of the state of maturity of olive-fruits [50], [51]. In this regard, it must be additionally highlighted that, even for any given tree, fruit ripening may vary depending to conditions such as its location within the tree or its degree of exposure to direct sunlight, among other. In order to illustrate this fact, Fig. 4 shows a set of four *Arbequina*-variety olive-fruits, all of them collected in the same orchard, and at the same time, where it can be appreciated the lack of uniformity in terms of colour between the fruits.

As a consequence of these facts, it can be concluded that colour variability induced by fruit maturity may be, at least, comparable to that induced by fruit variety. It is for this reason that colour features were discarded from the beginning, this is from image capture, so morphological characteristics of the fruits were explored as distinctive features for variety categorization.

As detailed in section III-B, fruits were photographed in batches of 50 individuals each. In addition, they were stochastically disposed over the capture area, enabling a scenario in which the fruits may appear touching each other. With the aim of making the methodology able to individually categorise every single olive-fruit present in the images, the first step of pre-processing is to transform initial captures into a suitable set of individual-fruit images.

The methodology proposed by [49] provides an efficient procedure for transforming the starting captures of multiples olive-fruits into binary images, where all the connected components corresponding to the different fruits are accurately separated. This method exploits the high contrast, in terms

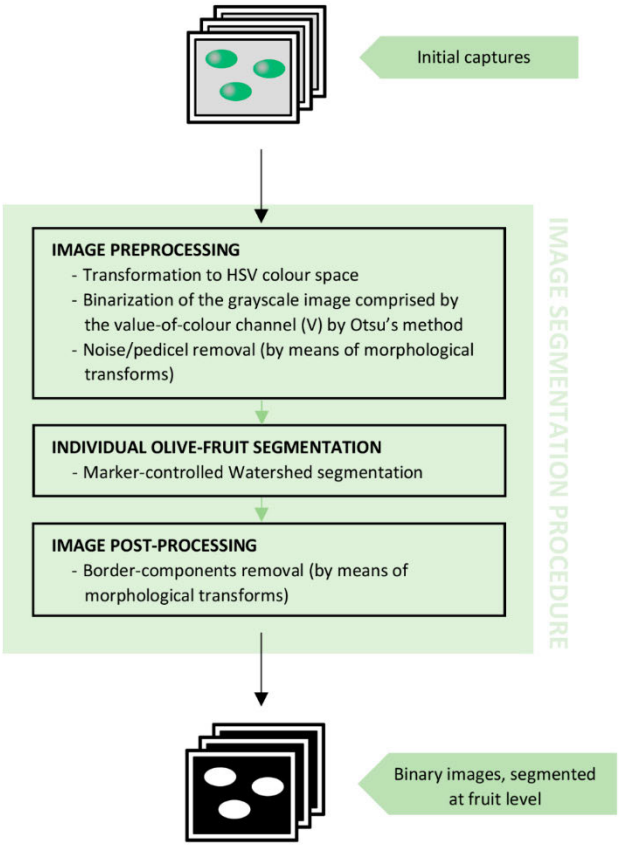

FIGURE 5. Representative diagram of the methodology proposed in [49] for the segmentation of the olive-fruits which appear in an image stochastically positioned.

of luminosity, between the fruits and background to perform the segmentation of the images. This latter, by discriminant analysis-based global thresholding [52]. After that, and by morphological analysis, the resulting binary images are transformed in order to yield a set of markers with which it is carried out an eventual marker-controlled Watershed segmentation [53]. This last step allows to separate those connected components which may appear wrongly fussed, for belonging to fruits that are touching each other in the original capture. Fig. 5 offers a diagram briefly describing this procedure. Fig. 6 shows the result of its application to one of the images initially acquired for this study.

Once images are binarized, and the contained components are correctly isolated by applying this methodology, each of them is extracted and individually included in a new square binary image of 501 pixels high and wide. It should be noted that each component is positioned at the centre, i.e., matching its centre of mass with the centre of the 501×501 frame. Hereafter, the rest of the processing is applied to these individual olive-fruit images.

As the generated images are binary, fruits appear as flat objects. The next step pursues to transform them into olive-fruits with a depth consistent with their shape. To do so, a weighing function based on the distance transform is applied, converting the binary images into a greyscale

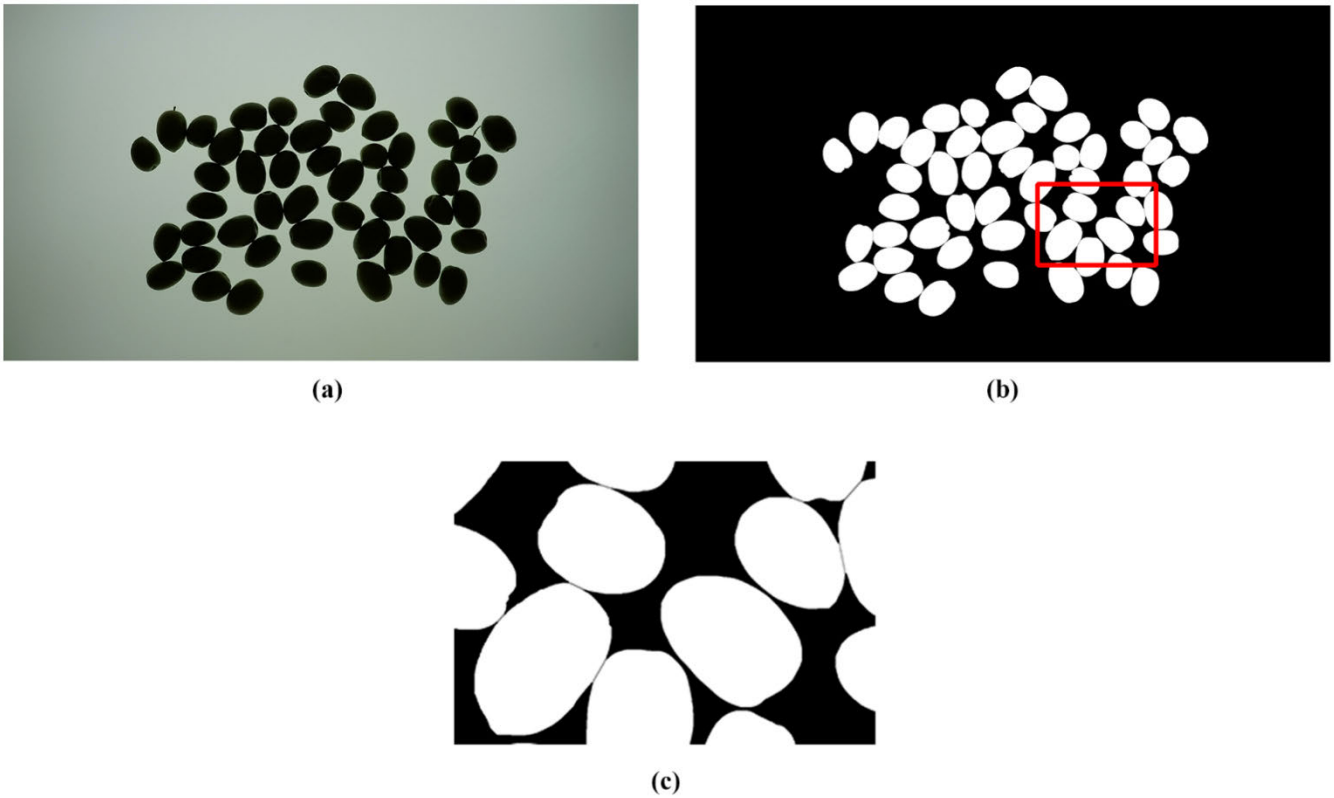

FIGURE 6. (a) Original image; (b) image (a) segmented according with the procedure proposed in [49]; (c) closeup of the red-squared area in image (b).

format. Hence, different grey level values are assigned to each olive-fruit pixel, thus providing the sphericity and three-dimensionality of the fruits [49]. So, being p a foreground pixel of a binary image f of 501×501 pixels in size which contains a single centred olive-fruit, the grey level value v_p assigned to p in the transform image can be computed as follows:

$$v_p = log_3(1 + 2 \times [D(f)](p)), \tag{1}$$

where D refers to the distance function [54] applied to image f, so the expression $[D(f)](p)$ can be defined as the Euclidean distance between p and the nearest background pixel, q. Mathematically:

$$[D(f)](p) = min\{d_\varepsilon(p, q) \,|\, f(q) = 0\}, \tag{2}$$

$$d_\varepsilon(p, q) = \sqrt{(p_x - q_x)^2 - (p_y - q_y)^2}. \tag{3}$$

where (p_x, p_y) and (q_x, q_y) are, respectively, the coordinates of the pixels p and q.

The entire process is illustrated in Fig. 7. Note that for the sake of facilitating the visualization of the partial results of the methodology, a sub-image of the original one, which contains a batch of 50 olive-fruits, is used. On the other hand, Fig. 8 shows examples of individual olive-fruit images obtained by the procedure proposed, for each of the varieties considered in the investigation.

B. IMAGE CLASSIFICATION

1) IMAGE DATASET ORGANIZATION

As commented before, the image dataset used throughout the experimentation was generated from photographs of 400 olive-fruits per variety. As proposed in section IV-A, initial captures were processed to obtain individual fruit images, yielding a total of 2,800 of them (400 per each of the seven varieties). 1,050 out of the 2,800 images (150 per variety) were kept for external validation, whereas the resting 1,750 images (250 per variety) were used for training the different CNNs. In order to increase this training dataset, a data augmentation based on image rotation was carried out.

Therefore, per single-fruit image belonging to the training set described hereabove, a rotation transform of 45° was applied. This transformation was repeated by using the resulting image, and so on until seven rotations were performed. Thus, seven extra images were yielded per fruit. Hence, in short, the 1,750 fruits (250 per variety), initially photographed in batches of 50, delivered 14,000 501 × 501 pixel-resolution images (2,000 per variety), each of them contains a single olive-fruit. On the other hand, it should be noted that the CNN architectures considered were implemented such that the input expected for all of them was 3-channel images. Since the methodology proposed is based on greyscale images, the image-structures obtained by the procedure described hereabove are triplicated and integrated

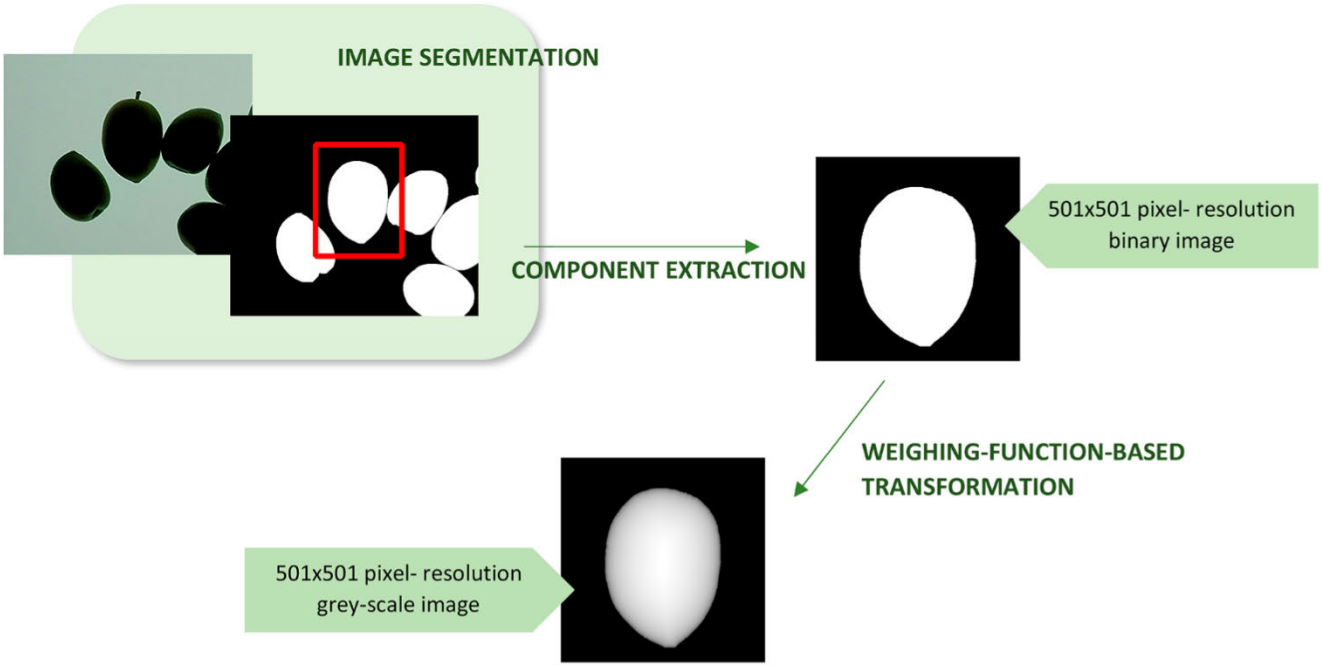

FIGURE 7. Representative diagram of the developed procedure for transforming the initial captures into a set of individual olive-fruit images.

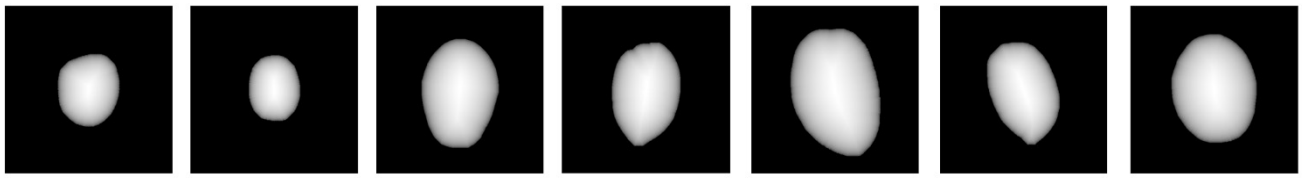

FIGURE 8. Examples of individual olive-fruit images obtained for each of the varieties under study, after transforming initial captures by the proposed procedure: (a) ***Arbequina*** variety; (b) ***Arbosana*** variety; (c) ***Changlot Real*** variety; (d) ***Lechín de Sevilla*** variety; (e) ***Ocal*** variety; (f) ***Picual*** variety; (g) ***Verdial de Huévar*** variety.

into the same file, so the final images are made up of three channels containing exactly the same information. Fig. 9 illustrates the data augmentation performed.

Table 1 summarizes, per variety, how the corresponding image dataset was organized.

2) CNN TRAINING

Implementations of the considered CNN architectures were trained in order to potentially perform the classification of the olive fruits. To that end, first, the 14,000 individual-fruit training images were appropriately labelled according to their variety. Then, as the CNN architectures were available pre-trained with the thousands of images contained in the ImageNet dataset [37], transfer learning [19] was accomplished to retain convolutional patterns a-priori 'known' by the nets. However, all implementations were modified in order to consider the right number of classification classes. Indeed, ImageNet contains labelled images from 1,000 categories, while the present study considers seven not included in that set, those in accordance with the olive cultivars under study. Therefore, the output layer was conveniently modified in all cases by reducing it to seven classification nodes.

Here below, Table 2 details the configuration parameters and the main training milestones for the different CNN architectures tried.

Each of the CNNs were trained during a different number of epochs, depending on the particularities of each architecture which makes them to converge to an optimum result at a different pace. This convergence was judged by analysing the partial results offered by the loss function evolution during training. In the same way, the mini-batch size used was not necessarily the same for the different architectures either. Indeed, this parameter was adapted to each specific case for optimising the learning time. It should also be noted that during training and before every epoch, the training-data was shuffled. When dividing the training dataset into mini-batches of a same given size, the division was not exact for any case, thus producing residual images not used in the learning

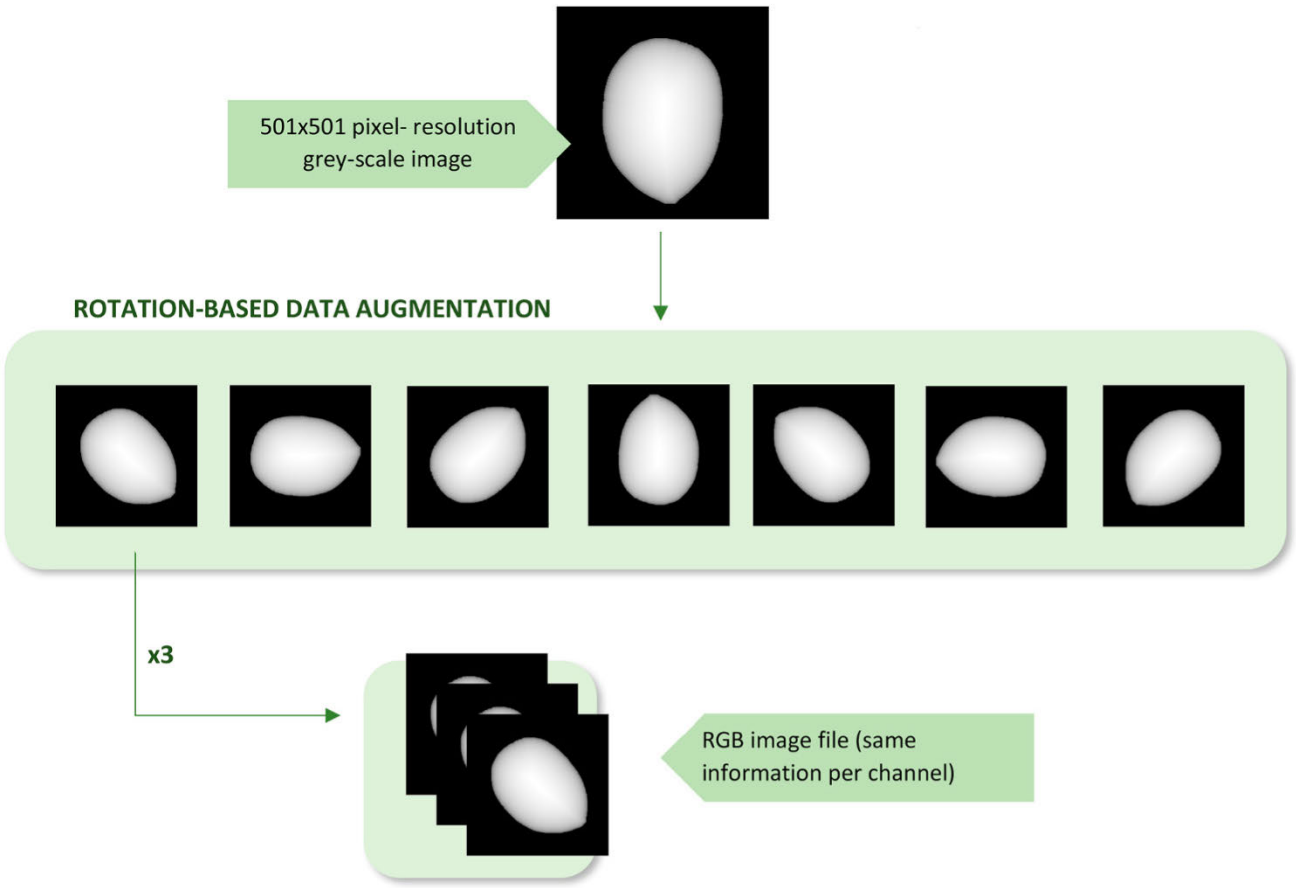

FIGURE 9. Representative diagram of the rotation-based data augmentation performed.

TABLE 1. Materials: organization of the image dataset.

	Number of fruits samples	Initial captures with multiple fruits	Individual-fruit images	Training individual-fruit images	Validation individual-fruit images
i-th variety	400	8[a]	400	2,000[b]	150
Total (7 varieties)	2,800	56[a]	2,800	14,000[b]	1,050

[a] 50 fruits per capture.
[b] After data augmentation.

process. Thanks to data shuffling, the residual images were substituted after every training epoch, thus exploiting the knowledge provided by the whole imagery.

Fig. 10 shows the three maximum filter responses produced by the five convolutional layers of AlexNet, after being trained, when it is excited with sub-image (a). It shows how the outer layers model gross distinctive features of the olive, whereas the inner ones focus on the subtle details. Regarding these last, note how the depth given to the fruit in the pre-processing is captured and exploited by the net for characterisation.

3) CNN VALIDATION

Once the networks were trained, they were tried in classifying the images corresponding to the external validation set. This, in order to assess the goodness of the models yielded after the training process.

The metric proposed for quantifying the performance of the classifiers was based on the ratio between the numbers of fruits correctly categorized within a specific variety, and the total number of them included in the corresponding validation subset. Mathematically:

$$HR_{CN,v} = \frac{h_{CN,v}}{N_v}, \tag{4}$$

where $h_{CN,v}$ is the number of olive-fruits of the variety v correctly categorized by the convolutional neural network CN, and N_v correspond to the total number of fruits (actually images of individual fruits) belonging to that variety, in the external validation set. N_v will be 1,050 in all cases.

TABLE 2. Summary of the configuration of the CNNs, and the main milestones registered from their training.

	AlexNet	InceptionV1	InceptionV3	ResNet-50	ResNet-101	Inception-ResNetV2
Epochs	168	85	67	50	77	74
Iterations	117,648	26,598	37,602	14,090	43,202	103,661
Mini-batch size	20	45	25	50	25	10
Input image size (pixels)	227×227	224×224	299×299	224×224	224×224	299×299
Learning rate	0.001	0.001	0.001	0.001	0.001	0.001

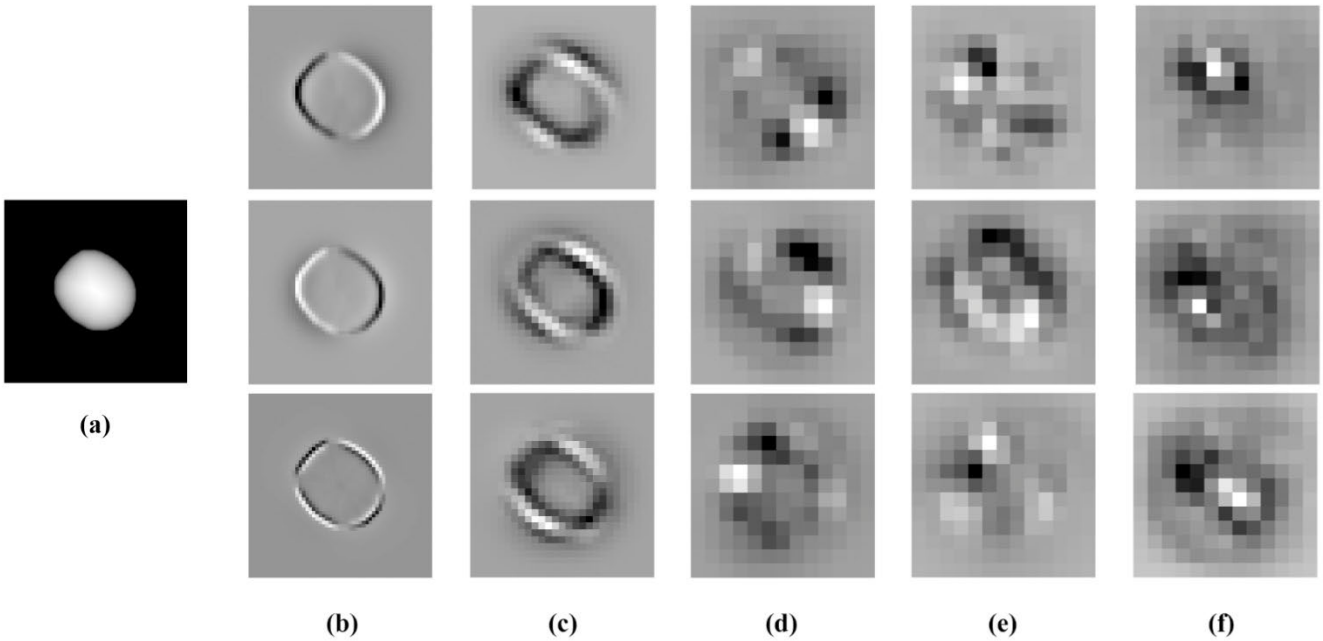

FIGURE 10. Representation of the three maximum filter responses produced by AlexNet to the input image (a); the net was trained with the set of 14,000 individuals kept to this effect. Responses follow the order of their corresponding layers, being (b) those from the outer layer and (f) from the inner. Note how finer details are characterised as the layer is deeper. Also, analyse how the depth given to the fruits in the pre-processing is exploited by the net, especially in the deeper layers, for fruit characterisation.

In addition, the average hit-rate obtained by each classifier, *CN*, is defined as follows:

$$HR_{CN} = \frac{\sum_v HR_{CN,v}}{\#v}, \tag{5}$$

where $\#v$ refers to the number of olive varieties (seven in the present case study).

V. RESULTS AND DISCUSSION

Table 3 shows the results, in terms of the metrics defined in (4) and (5), obtained with the six different CNN architectures. The results were measured from the classifications performed by the different CNNs for the total of 1,050 individual olive-fruit images in the external validation set.

As it can be checked, Inception-ResNetV2 offered the overall best results. Nevertheless, exclusively attending to these outcomes, the differences in terms of accuracy among the different architectures, maybe excepting that given by AlexNet, was not substantial enough to draw definitive conclusions regarding the supremacy of one of them for the case of study. Indeed, in general, performance of all classification models was remarkable, with an average accuracy above 90% in almost all cases.

For a certain image, the CNN output provides a probability value of belonging to each of the seven varieties. The higher the probability given of belonging to the correct class, the better the CNN was able to correctly recognise the variety. Table 4 details the average probability, of belonging to the correct class, and the corresponding standard deviation given by the different architectures when classifying the 150 images of each of the seven varieties; figures are also calculated considering images from all varieties as a whole. It can be identified that Inception-ResnetV2 also outperformed the other alternatives from this perspective; AlexNet was again the less accurate solution.

TABLE 3. CNN implementations tested accuracy, based on results obtained after classifying the images which integrate the external validation set.

Variety	CNN architecture					
	AlexNet ($HR_{CN,v}$)	Inception-ResnetV2 ($HR_{CN,v}$)	InceptionV1 ($HR_{CN,v}$)	InceptionV3 ($HR_{CN,v}$)	Resnet-50 ($HR_{CN,v}$)	Resnet-101 ($HR_{CN,v}$)
Arbequina	0.9333	0.9333	0.9467	0.9533	0.9400	0.9267
Arbosana	0.9133	0.9067	0.9467	0.9400	0.9133	1.0000
Changlot	0.8667	0.9400	0.9200	0.9600	0.9600	0.9333
Lechín	0.8333	0.8867	0.9267	0.9067	0.9200	0.9067
Picual	0.9467	0.8933	0.9600	0.9600	0.9400	0.9867
Ocal	0.9133	0.9333	0.9667	0.9933	0.9667	0.9733
Verdial	0.8867	0.9333	0.9733	0.9600	0.9400	0.9867
Overall	0.8990	0.9181	0.9486	0.9533	0.9400	0.9591

TABLE 4. Average ($\bar{x}$) and standard deviation (σ) of the probability of belonging to the correct class given by the different architectures, measured on the 150 images of each of the seven varieties, and also considering images from all varieties as a whole.

Variety	CNN architecture					
	AlexNet ($\bar{x}, \sigma$)	Inception-ResnetV2 ($\bar{x}, \sigma$)	InceptionV1 ($\bar{x}, \sigma$)	InceptionV3 ($\bar{x}, \sigma$)	Resnet-50 ($\bar{x}, \sigma$)	Resnet-101 ($\bar{x}, \sigma$)
Arbequina	(0.9283, 0.2241)	(0.9333, 0.2199)	(0.9280, 0.2240)	(0.9419, 0.2029)	(0.9477, 0.1910)	(0.9374, 0.2094)
Arbosana	(0.8913, 0.2605)	(0.9894, 0.0573)	(0.9081, 0.2632)	(0.9312, 0.2199)	(0.9342, 0.2007)	(0.9100, 0.2563)
Changlot	(0.8610, 0.3120)	(0.9183, 0.2404)	(0.9294, 0.2283)	(0.9075, 0.2319)	(0.9461, 0.1792)	(0.9561, 0.1583)
Lechín	(0.8270, 0.3448)	(0.9077, 0.2539)	(0.8767, 0.2880)	(0.9076, 0.2286)	(0.8990, 0.2371)	(0.8993, 0.2493)
Picual	(0.9293, 0.228)	(0.9743, 0.1154)	(0.8938, 0.2771)	(0.9465, 0.1762)	(0.9449, 0.1702)	(0.9339, 0.2135)
Ocal	(0.9001, 0.2665)	(0.9757, 0.1346)	(0.9318, 0.2244)	(0.9630, 0.1490)	(0.9701, 0.1005)	(0.9668, 0.1300)
Verdial	(0.8901, 0.2855)	(0.9738, 0.1046)	(0.9324, 0.2184)	(0.9637, 0.1314)	(0.9469, 0.1822)	(0.9639, 0.1409)
Overall	(0.8896, 0.2789)	(0.9532, 0.1783)	(0.9143, 0.2485)	(0.9373, 0.1961)	(0.9413, 0.1852)	(0.9382, 0.2011)

Thus, for the case of the images of *Arbosana*, the average probability of belonging to that variety provided by the net was 0.9894, with a very small standard deviation of 0.0573. This effect can be also found for the case of *Lechín*, *Picual*, *Ocal*, *Verdial* and considering all instances together. As with results from Table 3, differences were not so significant so as to take assertive conclusions. Notwithstanding, both sets of outcomes induce to analogous reflections.

It is worth noting that the CNN based on the AlexNet architecture, closely followed by the InceptionV1-based one, yielded the poorest results in both cases. The rest of CNNs performed better. To note that they all suppose a considerable increase of layers when compared with AlexNet and the first version of the Inception architecture. But nor this fact, neither the use of shortcuts-based architectures, as it happens in some of the cases (note that Resnet-50 yielded better results than Resnet-101), could necessary justify the better accuracy. At least more than the evidence that these four CNNs correspond to more recent and refined neural networks models. Hence, it should be necessary to undertake more research before stating the association between accuracy and the depth of the network. Be that as it may, such a homogeneous and general accurate result registered for all CNNs spotlights that the initial hypothesis of using the morphological modelling of the fruits as distinguishing characteristic is potentially valid. Indeed, given the reasons why colour features might not be appropriate to carry out an accurate variety categorization, the methodology proposed is potentially more suitable in order to achieve a more generalisable solution.

A contingency table is presented in Table 5 for the classifications performed by Inception-ResnetV2. As it can be observed, the net overestimated some classes and underestimated others. Of special interest is the analysis of the actual class *Arbequina*, where six of their images were wrongly

TABLE 5. Contingency table of the classification performed by Inception-ResnetV2 on the set of images for external validation.

Predicted class	Actual class							Predicted instances
	Arbequina	Arbosana	Changlot	Lechín	Picual	Ocal	Verdial	
Arbequina	139 (92.67%)	0 (0.0%)	0 (0.0%)	1 (0.67%)	0 (0.0%)	0 (0.0%)	0 (0.0%)	140
Arbosana	6 (4.0%)	150 (100%)	0 (0.0%)	1 (0.67%)	1 (0.67%)	0 (0.0%)	0 (0.0%)	158
Changlot	1 (0.67%)	0 (0.0%)	140 (93.33%)	2 (1.3%)	0 (0.0%)	1 (0.67%)	1 (0.67%)	145
Lechín	1 (0.67%)	0 (0.0%)	3 (2.0%)	136 (90.67%)	1 (0.67%)	0 (0.0%)	0 (0.0%)	141
Picual	0 (0.0%)	0 (0.0%)	4 (2.67%)	1 (0.67%)	148 (98.67%)	0 (0.0%)	0 (0.0%)	153
Ocal	2 (1.3%)	0 (0.0%)	0 (0.0%)	8 (5.3%)	0 (0.0%)	146 (97.33%)	1 (0.67%)	157
Verdial	1 (0.67%)	0 (0.0%)	3 (2.0%)	1 (0.67%)	0 (0.0%)	3 (2.0%)	148 (98.67%)	156
Actual instances	150	150	150	150	150	150	150	1050

classified as *Arbosana*. This phenomenon could be relevant if it would have also appeared in the contrary case, as it could indicate certain difficulty for the CNN to distinguish between both varieties. However, none of the *Arbosana* images were misclassified as being from *Arbequina*. A similar case occurred when attending to the actual class *Lechín*, as eight of its images were classified as *Ocal*. Notwithstanding, as for the previous case, there were not any images from *Ocal* classified as *Lechín*. This fact strengthen confidence in the capability of the net for discriminating among the different varieties thanks to the image pre-processing applied, and points to enrich the training set with more variability to obtain even better results.

VI. CONCLUSION

The purpose of this study was to assess the viability of a Computer Vision-based methodology to support the automatic and individual classification of olive-fruits, according to the variety they belong to. To that end, it was designed a procedure, based on image processing and analysis and CNNs, for developing a set of image classifiers. To the best to authors' knowledge, the presented algorithm is the first available proposal achieving that end in a non-invasive and accurate manner.

Hence, these image classifiers showed a remarkable behaviour in terms of performance, as high rates of accuracy were obtained in general for all of them, and in particular for the deeper CNN architectures. The outstanding accuracy found for all the different CNN architectures and versions, provides strong signs to validate the initial hypothesis of using morphological modelling of the fruits as distinctive varietal feature, at the expense of discarding colour characteristics.

Despite the quality of the results, further work may be approached by increasing the number of elements the neural networks were trained with. This, to the purpose of testing if it is possible to yield even better accuracy. Along the same lines, future research should include new olive cultivars in order to evaluate the goodness of the methodology proposed, as a general solution to the olive-fruit variety classification.

In addition, it should be underscored that the background the methodology proposed is based on, is aimed to satisfy real-time inspection of olive-fruits when they are transported on a real conveyor belt. By integrating the image processing procedure here presented to transform the initial captures of the fruits, and by applying the classification models computed, an integral solution could be built, potentially applicable to the olive sector, able to perform real time labelling of the olive-fruits, thus making possible their automatic grading and variety-based classification. Particularly, variety-based classification could have an important impact in reducing harvesting costs, as the need of sequentially processing collected fruits of a single variety at a time would disappear; by this way, harvesting could be organised by attending exclusively to the optimisation of operative costs. Additionally, the ability to classify olive-fruits in line could also have an impact in optimising the available space at the warehouse.

ACKNOWLEDGMENT

The authors would like to thank ''Virgen de la Oliva'' olive-oil cooperative for generously offering their orchards to conduct this work.

REFERENCES

[1] D. Kaniewski, E. Van Campo, T. Boiy, J.-F. Terral, B. Khadari, and G. Besnard, ''Primary domestication and early uses of the emblematic olive tree: Palaeobotanical, historical and molecular evidence from the Middle East,'' *Biol. Rev.*, vol. 87, no. 4, pp. 885–899, Nov. 2012.

[2] P. Vossen, ''Olive oil: History, production, and characteristics of the world's classic oils,'' *Amer. Soc. Horticultural Sci.*, vol. 42, no. 5, pp. 1093–1100, 2007.

[3] Word Table Olive Figures, International Olive Council (IOC). (2019). *World Statistics on Production, Imports, Exports and Consumption*. Accessed: Aug. 6, 2019. [Online]. Available: http://www.internationaloliveoil.org/estaticos/view/132-world-table-olive-figures

[4] Word Olive Oil Figures, International Olive Council (IOC). (2019). *World Statistics on Production, Imports, Exports and Consumption*. Accessed: Aug. 6, 2019. [Online]. Available: http://www.internationaloliveoil.org/estaticos/view/131-world-olive-oil-figures

[5] B. A. Keating, P. S. Carberry, P. S. Bindraban, S. Asseng, H. Meinke, and J. Dixon, "Eco-efficient agriculture: Concepts, challenges, and opportunities," *Crop Sci.*, vol. 50, pp. S-109–S-119, Mar. 2010.
[6] P. C. Struik and T. W. Kuyper, "Sustainable intensification in agriculture: The richer shade of green. A review," *Agronomy Sustain. Develop.*, vol. 37, no. 5, p. 39, Oct. 2017.
[7] H. C. J. Godfray, J. R. Beddington, I. R. Crute, L. Haddad, D. Lawrence, J. F. Muir, J. Pretty, S. Robinson, S. M. Thomas, and C. Toulmin, "Food security: The challenge of feeding 9 billion people," *Science*, vol. 327, no. 5967, pp. 812–818, Feb. 2010.
[8] L. Kitinoja, S. Saran, S. K. Roy, and A. A. Kader, "Postharvest technology for developing countries: Challenges and opportunities in research, outreach and advocacy," *J. Sci. Food Agricult.*, vol. 91, no. 4, pp. 597–603, Mar. 2011.
[9] A. Scheidel and F. Krausmann, "Diet, trade and land use: A socio-ecological analysis of the transformation of the olive oil system," *Land Policy*, vol. 28, no. 1, pp. 47–56, Jan. 2011.
[10] G. Giametta and B. Bernardi, "Olive grove equipment technology. Straddling trees: Mechanized olive harvests," *Adv. Horticultural Sci.*, vol. 24, no. 1, pp. 64–70, 2010.
[11] S. Naik and B. Patel, "Machine vision based fruit classification and grading—A review," *Int. J. Comput. Appl.*, vol. 170, no. 9, pp. 22–34, 2017.
[12] W. S. McCulloch and W. Pitts, "A logical calculus of the ideas immanent in nervous activity," *Bull. Math. Biophys.*, vol. 5, no. 4, pp. 115–133, Dec. 1943.
[13] F. Rosenblatt, "The perceptron, a perceiving and recognizing automaton," Cornell Aeronaut. Lab., Buffalo, NY, USA, Tech. Rep. 85-460-1, 1957.
[14] R. Raina, A. Madhavan, and A. Y. Ng, "Large-scale deep unsupervised learning using graphics processors," in *Proc. 26th Ann. Int. Conf. Mach. Learn.*, Montreal, QC, Canada, Jun. 2009, pp. 873–880.
[15] X.-W. Chen and X. Lin "Big data deep learning: Challenges and perspectives," *IEEE Access*, vol. 2, pp. 514–525, 2014.
[16] M. Bojarski, D. D. Testa, D. Dworakowski, B. Firner, B. Flepp, P. Goyal, L. D. Jackel, M. Monfort, U. Muller, J. Zhang, X. Zhang, J. Zhao, and K. Zieba, "End to end learning for self-driving cars," Apr. 2016, *arXiv:1604.07316*. [Online]. Available: https://arxiv.org/abs/1604.07316
[17] A. Shustanov and P. Yakimov, "CNN design for real-time traffic sign recognition," *Procedia Eng.*, vol. 201, pp. 718–725, Dec. 2017.
[18] D. Chaves, S. Saikia, L. Fernández-Robles, E. Alegre, and M. Trujillo, "Una revisión sistemática de métodos para localizar automáticamente objetos en imágenesc," *Revista Iberoamericana De Automática E Informática Ind.*, vol. 15, no. 3, pp. 231–242, Jun. 2018.
[19] H.-C. Shin, H. R. Roth, M. Gao, L. Le, Z. Xu, I. Nogues, J. Yao, D. Mollura, and R. M. Summers, "Deep convolutional neural networks for computer-aided detection: CNN architectures, dataset characteristics and transfer learning," *IEEE Trans. Med. Imag.*, vol. 35, no. 5, pp. 1285–1298, May 2016.
[20] S. Pereira, A. Pinto, V. Alves, and C. A. Silva, "Brain tumor segmentation using convolutional neural networks in MRI images," *IEEE Trans. Med. Imag.*, vol. 35, no. 5, pp. 1240–1251, May 2016.
[21] A. Kamilaris and F. X. Prenafeta-Boldú, "Deep learning in agriculture: A survey," *Comput. Electron. Agricult.*, vol. 147, pp. 70–90, Aug. 2018.
[22] D. I. Patrício and R. Rieder, "Computer vision and artificial intelligence in precision agriculture for grain crops: A systematic review," *Comput. Electron. Agricult.*, vol. 153, pp. 69–81, Oct. 2018.
[23] M. Rahnemoonfar and C. Sheppard, "Deep count: Fruit counting based on deep simulated learning," *Sensors*, vol. 17, no. 4, p. 905, 2017.
[24] A. Aquino, B. Millan, M.-P. Diago, and J. Tardaguila, "Automated early yield prediction in vineyards from on-the-go image acquisition," *Comput. Electron. Agricult.*, vol. 144, pp. 26–36, Jan. 2018.
[25] A. Aquino, M. P. Diago, B. Millán, and J. Tardáguila, "A new methodology for estimating the grapevine-berry number per cluster using image analysis," *Biosyst. Eng.*, vol. 156, pp. 80–95, Apr. 2017.
[26] B. Millan, A. Aquino, M. P. Diago, and J. Tardaguila, "Image analysis-based modelling for flower number estimation in grapevine," *J. Sci. Food Agricult.*, vol. 97, no. 3, pp. 784–792, Feb. 2017.
[27] L. A. da Silva, P. O. Bressan, D. N. Gonçalves, D. M. Freitas, B. B. Machado, and W. N. Gonçalves, "Estimating soybean leaf defoliation using convolutional neural networks and synthetic images," *Comput. Electron. Agricult.*, vol. 156, pp. 360–368, Jan. 2019.
[28] T. R. Chavan and A. V. Nandedkar, "AgroAVNET for crops and weeds classification: A step forward in automatic farming," *Comput. Electron. Agricult.*, vol. 154, pp. 361–372, Nov. 2018.
[29] G. Saleem, M. Akhtar, N. Ahmed, and W. S. Qureshi, "Automated analysis of visual leaf shape features for plant classification," *Comput. Electron. Agricult.*, vol. 157, pp. 270–280, Feb. 2019.
[30] Z. Dong, X. Chen, W. Jia, S. Du, K. Muhammad, and S.-H. Wang, "Image based fruit category classification by 13-layer deep convolutional neural network and data augmentation," *Multimedia Tools Appl.*, vol. 78, no. 3, pp. 3613–3632, 2019.
[31] F. J. Rodríguez, A. García, P. J. Pardo, F. Chávez, and R. M. Luque-Baena, "Study and classification of plum varieties using image analysis and deep learning techniques," *Prog. Artif. Intell.*, vol. 7, no. 2, pp. 119–127, 2018.
[32] S. S. Martínez, D. M. Gila, A. Beyaz, J. G. Ortega, and J. G. García, "A computer vision approach based on endocarp features for the identification of olive cultivars," *Comput. Electron. Agricult.*, vol. 154, pp. 341–346, Nov. 2018.
[33] P. Vanloot, D. Bertrand, C. Pinatel, J. Artaud, and N. Dupuy, "Artificial vision and chemometrics analyses of olive stones for varietal identification of five French cultivars," *Comput. Electron. Agric.*, vol. 102, pp. 98–105, Mar. 2014.
[34] A. Beyaz, M. T. özkaya, and D. Içen, "Identification of some spanish olive cultivars using image processing techniques," *Sci. Horticulturae*, vol. 225, pp. 286–292, Nov. 2017.
[35] W. Liu, Z. Wang, X. Liu, N. Zeng, Y. Liu, and F. E. Alsaadi, "A survey of deep neural network architectures and their applications," *Neurocomputing*, vol. 234, pp. 11–26, Apr. 2017.
[36] A. Voulodimos, N. Doulamis, A. Doulamis, and E. Protopapadakis, "Deep learning for computer vision: A brief review," *Comput. Intell. Neurosci.*, vol. 2018, Feb. 2018, Art. no. 7068349.
[37] J. Deng, W. Dong, R. Socher, L.-J. Li, K. Li, and L. Fei-Fei, "ImageNet: A large-scale hierarchical image database," in *Proc. IEEE Conf. Comput. Vis. Pattern Recognit.*, Jun. 2009, pp. 248–255.
[38] G. E. Hinton, N. Srivastava, A. Krizhevsky, I. Sutskever, and R. R. Salakhutdinov, "Improving neural networks by preventing co-adaptation of feature detectors," Tech. Rep. 001, Jul. 2012.
[39] Y. LeCun, Y. Bengio, and G. Hinton, "Deep learning," *Nature*, vol. 521, pp. 436–444, May 2015.
[40] G. Kumar and P. K. Bhatia, "A detailed review of feature extraction in image processing systems," in *Proc. 4th Int. Conf. Adv. Comput. Commun. Technol.*, Feb. 2014, pp. 5–12.
[41] J. Gu, Z. Wang, J. Kuen, L. Ma, A. Shahroudy, B. Shuai, T. Liu, X. Wang, G. Wang, J. Cai, and T. Chen, "Recent advances in convolutional neural networks," *Pattern Recognit.*, vol. 77, pp. 354–377, May 2018.
[42] A. Krizhevsky, I. Sutskever, and G. E. Hinton, "Imagenet classification with deep convolutional neural networks," in *Proc. Adv. Neural Inf. Process. Syst. (NIPS)*, 2012, pp. 1097–1105.
[43] C. Szegedy, W. Liu, Y. Jia, P. Sermanet, S. Reed, D. Anguelov, D. Erhan, V. Vanhoucke, and A. Rabinovich, "Going deeper with convolutions," in *Proc. IEEE Conf. Comput. Vis. Pattern Recognit. (CVPR)*, Jun. 2015, pp. 1–9.
[44] C. Szegedy, V. Vanhoucke, S. Ioffe, J. Shlens, and Z. Wojna, "Rethinking the Inception Architecture for Computer Vision," in *Proc. IEEE Conf. Comput. Vis. Pattern Recognit. (CVPR)*, Jun. 2016, pp. 2818–2826.
[45] K. He, X. Zhang, S. Ren, and J. Sun, "Deep residual learning for image recognition," in *Proc. IEEE Conf. Comput. Vis. Pattern Recognit. (CVPR)*, Jun. 2016, pp. 770–778.
[46] R. Pascanu, T. Mikolov, and Y. Bengio, "On the difficulty of training recurrent neural networks," in *Proc. 30th Int. Conf. Mach. Learn.*, Feb. 2013, pp. 1310–1318.
[47] S. Hochreiter, "The vanishing gradient problem during learning recurrent neural nets and problem solutions," *Int. J. Uncertainty, Fuzziness Knowl.-Based Syst.*, vol. 6, no. 2, pp. 107–116, 2003.
[48] C. Szegedy, S. Ioffe, V. Vanhoucke, and A. Alemi, "Inception-v4, inception-ResNet and the impact of residual connections on learning," Feb. 2016, *arXiv:1602.07261*. [Online]. Available: https://arxiv.org/abs/1602.07261
[49] J. M. Ponce, A. Aquino, B. Millan, and J. M. Andújar, "Automatic counting and individual size and mass estimation of olive-fruits through computer vision techniques," *IEEE Access*, vol. 7, pp. 59451–59465, 2019.
[50] M. Bouaziz, M. Chamkha, and S. Sayadi, "Comparative study on phenolic content and antioxidant activity during maturation of the olive cultivar Chemlali from tunisia," *J. Agricult. Food Chem.*, vol. 52, no. 17, pp. 5476–5481, 2004.
[51] G. Menz and F. Vriesekoop, "Physical and chemical changes during the maturation of Gordal Sevillana olives (Olea europaea L., cv. Gordal Sevillana)," *J. Agricult. Food Chem.*, vol. 58, pp. 4934–4938, Mar. 2010.

[52] N. Otsu, "A threshold selection method from gray-level histograms," *IEEE Trans. Syst., Man, Cybern.*, vol. 9, no. 1, pp. 62–66, Jan. 1979.
[53] R. C. Gonzalez and R. E. Woods, *Digital Image Processing*, 4th ed. New York, NY, USA: Pearson, 2018.
[54] P. Soille, *Morphological Image Analysis: Principles and Applications*. Berlin, Germany: Springer, 2004.

JUAN M. PONCE was born in Huelva, Andalusia, Spain, in 1982. He received the Engineering degree in computers science from the University of Seville, Seville, in 2009. He is currently pursuing the Ph.D. degree in image analysis with the University of Huelva, Huelva.

After performing different jobs within the software development industry as a Programmer and an Analyst, nowadays he is with the University of Huelva. His research interest includes developing computer-vision-based technology, potentially applicable in food industry and precision agriculture.

ARTURO AQUINO was born in Huelva, Andalusia, Spain, in 1982. He received the Engineering degree in computer science from the University of Seville, in 2006, the M.Sc. degree in computer engineering and networks from the University of Granada, in 2007, and the Ph.D. degree in image analysis from the University of Huelva, in 2011.

Since 2007, he has been with various academic posts at the University of Granada, the University of Huelva, the Research Centre for Mathematical Morphology, Mines ParisTech, and the University of La Rioja. He is currently a Postdoctoral Researcher and a Lecturer with the University of Huelva. Until 2019, he has published more than 40 papers, including articles, book chapters, and contributions to conferences, and he holds two patents. He has directed a doctoral thesis and has participated in eight European, national, and regional research projects. His research interests include image analysis, processing, and understanding.

JOSÉ M. ANDÚJAR was born in Huelva, Spain. He received the Ph.D. degree, in 2000. He is currently a Full Professor of systems engineering and automatic control with the University of Huelva, Spain. Throughout his professional life, he has received 24 awards and academic honors. He has conducted ten doctoral theses with eight prizes, and he holds 12 international patents. He has more than 100 articles published in indexed journals in the ISI Journal Citation Reports. Specifically, he has 51 quartile Q1 publications in 20 different journals; most of these are among the top 10 in their categories, and several are number 1. He has led or co-led more than 50 research projects funded by public institutions and companies. His main research interests include control engineering, renewable energy systems, remote piloted aircraft systems applications, and engineering education.